Epithelial hedgehog signals pattern the intestinal crypt-villus axis

Blair B. Madison, Katherine Braunstein, Erlene Kuizon, Kathleen Portman, Xiaotan T. Qiao and Deborah L. Gumucio*

Department of Cell and Developmental Biology, University of Michigan Medical School, Ann Arbor, MI 48109-0616, USA
*Author for correspondence (e-mail: dgumucio@umich.edu)

Accepted 9 November 2004

Development 132, 279-289
Published by The Company of Biologists 2005
doi:10.1242/dev.01576

Summary

Morphological development of the small intestinal mucosa involves the stepwise remodeling of a smooth-surfaced endodermal tube to form finger-like luminal projections (villi) and flask-shaped invaginations (crypts). These remodeling processes are orchestrated by instructive signals that pass bidirectionally between the epithelium and underlying mesenchyme. Sonic (Shh) and Indian (Ihh) hedgehog are expressed in the epithelium throughout these morphogenic events, and mice lacking either factor exhibit intestinal abnormalities. To examine the combined role of Shh and Ihh in intestinal morphogenesis, we generated transgenic mice expressing the pan-hedgehog inhibitor, Hhip (hedgehog interacting protein) in the epithelium. We demonstrate that hedgehog (Hh) signaling in the neonatal intestine is paracrine, from epithelium to Ptch1-expressing subepithelial myofibroblasts (ISEMFs) and smooth muscle cells (SMCs). Strong inhibition of this signal compromises epithelial remodeling and villus formation. Surprisingly, modest attenuation of Hh also perturbs villus patterning. Desmin-positive smooth muscle progenitors are expanded, and ISEMFs are mislocalized. This mesenchymal change secondarily affects the epithelium: Tcf4/β-catenin target gene activity is enhanced, proliferation is increased, and ectopic precrypt structures form on villus tips. Thus, through a combined Hh signal to underlying ISEMFs, the epithelium patterns the crypt-villus axis, ensuring the proper size and location of the emerging precrypt compartment.

Key words: Hedgehog, Wnt, Intestine, Epithelial-mesenchymal crosstalk, Mouse

Introduction

By day E9.0 in the mouse, a tubular gut has formed and the endodermal epithelial lining is morphologically similar from end to end. Over the next five weeks, complex patterning events generate regionally distinct domains characteristic of the adult tubular gut: esophagus, stomach, duodenum, jejunum, ileum, cecum, and colon (Cheng and Bjerknes, 1985; Mathan et al., 1976; Wells and Melton, 1999). Tissue recombination studies have shown that the overall instructions for this regional pattern are dictated by soluble signals that pass between the epithelium and the surrounding mesenchyme (reviewed by Kedinger et al., 1998).

In the small intestine, this inter-tissue communication is first visible at E14.5. At this time, under the influence of the mesenchyme, the stratified squamous epithelium is remodeled to form intestinal villi lined with a single layer of columnar epithelium (Mathan et al., 1976). Morphological evidence of patterning along the crypt-villus axis is seen by E16.5 (Calvert and Pothier, 1990), when proliferative cells become concentrated in the flat intervillus regions that will later postnatally give rise to the crypts, the eventual home of intestinal stem cells. Studies indicate that crypt development proceeds by anchorage of prospective stem cells to the intervillus region and remodeling of the villus above these anchored cells to form flask-shaped crypt structures (Calvert and Pothier, 1990), but the signals responsible for the selective localization of the precrypt structures at the base of the villi have not been identified. The mechanical process of crypt formation may be assisted by the action of the contractile subepithelial pericryptal myofibroblasts, or ISEMFs (Powell et al., 1999). ISEMFs are thought to exist as a syncytium of cells, concentrated in the crypt regions and extending into villus tips where they merge with pericytes (Powell et al., 1999). In addition to their probable mechanical action in shaping the crypts, ISEMFs are a major source of instructive signals to the epithelium, and are capable of promoting epithelial proliferation or differentiation via soluble and/or membrane-tethered signals (Kedinger et al., 1998). Alterations in the character and/or distribution of ISEMFs are associated with several intestinal pathologies, including Crohn's disease and adenomatous colorectal polyps (Adegboyega et al., 2002; Andoh et al., 2002).

Both the hedgehog (Hh) and Wnt signaling pathways are likely to play important roles in intestinal crypt-villus axis formation and stem cell homeostasis. Several Wnt proteins, as well as their Frizzled receptors, are expressed in both epithelial and mesenchymal compartments (Theodosiou and Tabin, 2003). Tcf4 (*Tcf7l2*), a transcriptional effector of Wnt signals, is localized to the intervillus epithelium as early as E16.5 (Korinek et al., 1998). Mice lacking Tcf4 exhibit fewer villi, and severely reduced proliferation in the intervillus regions (Korinek et al., 1998), evidence that Tcf4 is required for establishment and/or maintenance of the crypt stem cell population. Furthermore, proliferation in the intestinal crypt compartment is Wnt ligand dependent (Pinto et al., 2003). Interrupting Wnt signals by expression of a pan-Wnt inhibitor

(*Dkk1*) in the intestine profoundly reduces epithelial proliferation. This is accompanied by decreased *Myc* expression and increased expression of the cell cycle inhibitor, *p21* (*Cdkn1a/Cip1/Waf1*). Thus, Wnt ligands control a master switch between proliferation and differentiation along the crypt-villus axis (van de Wetering et al., 2002).

Sonic (Shh) and Indian (Ihh) hedgehog proteins also play important roles in small intestinal morphogenesis. Initially expressed throughout the epithelium, both proteins are redistributed after villus formation, becoming concentrated in cells of the intervillus region (Ramalho-Santos et al., 2000). Mice deficient in *Shh* or *Ihh* display extensive gastrointestinal phenotypes (Ramalho-Santos et al., 2000). $Ihh^{-/-}$ mice die perinatally and exhibit reduced proliferation in the intervillus region, leading to a depleted progenitor cell compartment (Ramalho-Santos et al., 2000), suggesting that *Ihh* is critical for the maintenance of intestinal stem cells. Interestingly, $Shh^{-/-}$ mice display the opposite phenotype: overgrowth of duodenal villi (and stomach epithelium). This implies that *Shh* may inhibit rather than stimulate proliferation in these regions (Ramalho-Santos et al., 2000). Though the epithelial phenotypes of *Shh* vs. *Ihh* null mice are disparate, both models exhibit reduced smooth muscle, suggesting that these two hedgehog signals also have partially redundant functions.

The goal of the work described here was to explore the role of the combined Shh and Ihh signal in late intestinal development. Since mice doubly deficient for *Shh* and *Ihh* do not develop past early somite stages, we engineered an intestine-specific blockade of Hh signals by overexpression of the pan-Hh inhibitor, Hhip. We find that even minor reductions in Hh signals are sufficient to produce a robust increase in epithelial proliferation. The epithelial effect of Hh perturbation is indirect since our data indicate that Hh signals are paracrine and impact ISEMFs and smooth muscle cells (SMCs). When Hh signals are reduced, ISEMFs, a potential source of Wnt signals (Brittan and Wright, 2004), are abnormally located in villus tips in association with proliferating epithelial cells that express high levels of Tcf4/β-catenin target genes. Thus, the dose of the Hh signal to ISEMFs is normally under tight control; through this signal the epithelium indirectly regulates the size and location of its own proliferative compartment, effectively controlling the organized patterning of the crypt-villus axis.

Materials and methods

Transgene preparation, injection, and founder analysis

A truncated version of the *Hhip* cDNA (lacking the C-terminal transmembrane domain, *HhipΔTM*) was isolated by RT-PCR of cDNA from E12.5 whole embryo RNA and cloned into pBSII-SK+ (Stratagene), 3′ of the 12.4 Kb mouse villin (Vil1) promoter (Madison et al., 2002), and 5′ of a bovine *GH1* polyA signal. The vector backbone was removed prior to microinjection of C57BL6/SJL or C57BL6 fertilized oocytes. PCR genotyping of tail DNA was used to identify transgenic founders. Founders were used in all analyses, except where otherwise noted. Three separate injections yielded 18 individual founders for analysis. Founders 1-8 were analyzed by Q-RT-PCR, histology, Ki67 analysis, and immunostaining for specific proteins, while founders 9-14 were processed for histology and Ki67 analysis only. Founders 15-18 were transgene positive, but did not exhibit a phenotype. Wild-type littermates were used as controls.

Villin-noggin transgenic production and immunohistochemistry

The noggin cDNA was amplified by RT-PCR of E12.5 C57BL/6 whole mouse embryo RNA, TOPO cloned into pCR2.1-TOPO (Invitrogen), and the sequence was verified. The plasmid was digested with SacII and ApaI and cloned into pBSII-SK+ (Stratagene) digested with SacII and XbaI to create pBSII-noggin. This was digested with SacII and KpnI to remove the cDNA and cloned into SacII and KpnI sites 3′ of the 12.4Kb villin promoter/enhancer fragment (Madison et al., 2002) and 5′ of an SV40 polyadenylation sequence from the pGL2-basic (Promega) plasmid to create the p12.4KVil-noggin plasmid with a puc18 backbone for growth in *E. Coli.* The transgene fragment was excised by digestion with PmeI and injected into pronuclei of C57BL6/SJL fertilized oocytes. PCR genotyping of tail DNA was used to identify transgenic founders. Fourteen founders were identified, and ten expressed the transgene mRNA.

Protein expression in founders was evaluated by immunohistochemistry for noggin protein using goat anti-noggin antiserum (R&D Systems, 1:250). Immunohistochemistry was performed on 6 μm paraffin sections. Sections were de-paraffinized, rehydrated, and non-specific peroxidase activity was blocked for 30 minutes in 1.5% H_2O_2 in PBS. Antigen retrieval was performed by boiling for 10 minutes in 0.01 M sodium citrate buffer, pH 6.0, and cooling on ice for 15 minutes. Immunostaining was performed using the TSA-biotin system (Perkin Elmer), and staining developed with SigmaFast DAB (Sigma).

Epithelial-mesenchymal separation of E18.5 embryonic small intestine

Small intestines from E18.5 C57BL/6 embryos were opened longitudinally and incubated for 8 hours in Cell Recovery Solution (BD Pharmingen) at 4°C. Gentle shaking separated the epithelium from the mesenchyme. The mesenchyme was removed with tweezers and homogenized in 1 ml of TRIzol (Invitrogen) to prepare RNA. The epithelium was pelleted by centrifugation, and resuspended in 1 ml of TRIzol. Using the iScript cDNA synthesis kit (Biorad), cDNA was synthesized from 1 μg of total epithelial or mesenchymal RNA. To detect expressed genes, PCR was performed for 30 cycles using primers indicated in Table S1 in the supplementary material.

ISEMF cell culture

Rat intestinal ISEMF cell lines MIC101, MIC216, and MIC316 were obtained from Dr Michele Kedinger (INSERM, Strasbourg, France) and cultured in DMEM-F12 nutrient mixture, with 10% fetal bovine serum (FBS) at 37°C, 5% CO_2. The human colonic ISEMF cell line CCD-18Co (ATCC, #CRL-1459) was cultured according to ATCC specifications. Shh-conditioned medium was prepared by Fugene (Roche) transfection of Cos7 cells (maintained in DMEM, 10% FBS) with 4 μg of pcDNA3.1 or pcDNA3.1-Shh expression plasmid per 10 cm plate. The pcDNA3.1-Shh expression vector was obtained by cloning the full-length cDNA for *Shh* (obtained by RT-PCR of E18.5 small intestine RNA) into an EcoR1 site in pcDNA3.1 by standard techniques. Eighteen hours after transfection, Cos7 medium was replaced with medium specific to each ISEMF cell line and incubated for 30 additional hours. Conditioned medium was filtered through a 0.22 μm filter and stored at –80°C. ISEMF cell lines grown in six-well plates were treated with conditioned medium for 24 and 72 hours. During the 72-hour incubation, fresh conditioned medium was added after 48 hours. Medium was then aspirated, RNA prepared using TRIzol, and cDNA synthesized as described above. All tissue reagents are from Invitrogen Corporation, unless indicated otherwise.

E18.5 intestinal mesenchyme culture and stimulation with Shh-N

Small intestines from E18.5 C57BL/6 embryos were opened longitudinally and incubated for 8 hours in Cell Recovery Solution (BD Pharmingen) at 4°C. Gentle shaking separated the epithelium

from the mesenchyme. The mesenchyme was removed with tweezers, finely minced with a scalpel, and cultured on collagen-coated 12-well plates in DMEM, 10% FBS, 10 mM Hepes. Medium was changed after 24 hours, replaced with new medium, and cultured for an additional 24 hours. Tissue was then treated for 12, 36, or 48 hours with 0.1, 0.5, or 2.5 μg/ml recombinant mouse Shh N-terminal polypeptide (Shh-N, R&D Systems) or equivalent amount of vehicle (5% trehalose, 12.5 mg/ml BSA, in PBS). All reagents were obtained from Invitrogen Corporation, unless stated otherwise.

Histology, immunohistochemistry, immunofluorescence, and in situ hybridization

Standard histological procedures were used for H and E staining, Alcian Blue staining, and Oil Red-O staining. X-gal stain of *Ptch1*$^{+/nLacZ}$ neonatal jejunum was performed on cryostat sections as previously described (Madison et al., 2002). For subsequent α-smooth muscle actin (α-SMA) and desmin immunofluorescence, slides were washed three times with PBS and incubated overnight with mouse Cy3-conjugated anti-α-SMA, (Sigma, 1:500) and rabbit anti-desmin (AbCam, 1:250), followed by incubation with goat anti-rabbit Alexafluor 488 (Molecular Probes, 1:1000). *Ptch1*$^{+/nLacZ}$ mice are from Jackson Laboratories, strain B6;129-Ptch$^{tm1Mps/J}$, #003081.

Immunohistochemistry was performed on 6 μm paraffin sections. Sections were de-paraffinized, rehydrated, and nonspecific peroxidase activity blocked for 30 minutes in 1.5% H_2O_2 in PBS. Antigen retrieval was performed by boiling for 10 minutes in 0.01 M sodium citrate buffer, pH 6.0, and cooled on ice for 15 minutes. Immunostaining was performed using the TSA-biotin system (Perkin Elmer), and developed with SigmaFast DAB (Sigma). Antibodies used were: mouse anti-Hh (Developmental Studies Hybridoma Bank, clone 5E1, 1:1000), goat anti-Hhip (Santa Cruz, 1:50), rabbit anti-Ki67 (Novocastra, 1:3000), rabbit anti-Cdx1 (courtesy of Dr Debra Silberg, 1:500), goat anti-EphB2 (R&D Systems, 1:50), rat anti-CD44v6 (Bender MedSystems, 1:1000), rabbit anti-iFABP (courtesy of Dr Jeffrey Gordon, 1:400), rabbit anti-Chromogranin A (ImmunoStar, 1:10,000).

For α-SMA, Ki67, and desmin immunofluorescence, 6 μm paraffin sections were prepared as described above. Sections were blocked for 30 minutes at room temperature with 10% goat serum, 1% BSA, and 0.3% Triton-X 100, in PBS. Cy3-conjugated mouse anti-α-SMA (Sigma, 1:500), rabbit anti-Ki67 (Novocastra, 1:1000), and rabbit anti-desmin (Abcam, 1:250) were incubated overnight at 4°C, followed by incubation with goat anti-rabbit Alexafluor 488 (Molecular Probes, 1:1000).

Frozen sections were prepared by freezing tissue in OCT (TissueTek), sectioning at 4 μm, and fixing for 5 minutes in ice-cold 4% formaldehyde in PBS. The following antibodies were used: mouse anti-β-catenin (Transduction Laboratories, 1:1000), rabbit anti-CCK (Chemicon, 1:1000), rabbit anti-peripherin (Chemicon, 1:1000), rabbit anti-cGKII (courtesy of Dr Michael Uhler, 1:500), and Phalloidin-FITC (Molecular Probes, 1:250). Fluorophore-labeled secondary antibodies used were goat anti-rabbit Alexafluor 568 and goat anti-mouse Alexafluor 488 (Molecular Probes, 1:1000).

For in situ hybridization, a digoxigenin-labeled cRNA probe was created from a 959 bp cDNA fragment of the Ihh mRNA (nucleotides 828-1786, NCBI Accession Number BC046984) covering the exon 2-3 boundary and part of the 3′ UTR, and hybridized at 100-200 ng/μl on 10 μM cryosections from E18.5 C57BL/6 intestinal tissue. All other procedures were performed as described (Prado et al., 2004).

Quantitative RT-PCR analysis (Q-RT-PCR)

Cultured intestinal mesenchyme or whole tissue from wild-type or transgenic jejunum was homogenized in TRIzol (Invitrogen). Using the iScript cDNA synthesis kit (Biorad), cDNA was synthesized from 1 μg of total RNA. Q-RT-PCR was performed using SybrGreen incorporation on a BioRad iCycler using primers listed in Table S1 (see supplementary material). Threshold cycles were normalized to threshold cycles for *HPRT*.

Results

Hh signals in neonatal intestine are paracrine

Previous data indicate that during mid- to late fetal life, *Shh* and *Ihh* are expressed in the small intestinal epithelium while the Hh receptors (*Ptch1*, *Ptch2*), the downstream transcription factor, *Gli1*, as well as the Hh target gene *Bmp4* are expressed in the mesenchyme (Motoyama et al., 1998; Ramalho-Santos et al., 2000; Sukegawa et al., 2000; Wang et al., 2002). However, recent studies in adult colon indicate that the *Ptch1* receptor is expressed throughout the epithelium and in scattered stromal cells (van den Brink et al., 2004), indicating that Hh signaling in the large intestine can be autocrine or paracrine. Here we used several approaches to clearly establish the direction of the Hh signal in the neonatal small intestine. In situ hybridization shows that *Ihh* expression is limited to the intervillus region at the base of the villi (Fig. 1A). Though we could not detect *Shh* by in situ hybridization, RT-PCR confirms that this message is present only in epithelium (see below). Examination of Hh protein distribution, using an antibody that detects both Ihh and Shh, reveals Hh protein concentrated in the subepithelial region at the base of the villi (Fig. 1B). Finally, we examined the expression of *Ptch1*, as detected by X-gal staining in *Ptch1*$^{+/nLacZ}$ mice (Goodrich et al., 1997). Since *Ptch1* is both the receptor for Hh signals and a direct target gene, its expression domain is a direct indication of the cellular targets of Hh signaling. No expression of LacZ from the *Ptch1* locus is detected in the epithelium, indicating that autocrine signaling does not occur in the neonatal small intestine. LacZ staining is most prominent in fibroblast-like cells located immediately beneath the epithelium near the base of villi (Fig. 1C). Some expression is also seen in scattered cells in the cores of the villus tip lamina propria, suggesting that Hh proteins may be capable of both short- and long-range signaling along the developing crypt-villus axis. Alternatively, or additionally, the scattered distribution of β-galactosidase-positive cells may reflect the syncytial organization of some lamina propria fibroblasts (Powell et al., 1999). Finally, weak staining is observed in the innermost layer of the muscularis externa (ME) (Fig. 1C, arrowhead). The β-galactosidase staining pattern in *Gli1*$^{+/nLacZ}$ mice is identical to these findings in *Ptch1*$^{+/nLacZ}$ mice (B. B. Madison, unpublished).

To confirm the paracrine direction of Hh signals, epithelial and mesenchymal components of E18.5 intestine were separated (Fig. 1D,E) and the purity of each fraction was assayed by RT-PCR for specific genes known to be restricted to epithelium (villin) or mesenchyme (*Actg2* and *Madcam1*) (Fig. 1F). Very low levels of gamma smooth muscle actin (*Actg2*) mRNA in the epithelial fraction may reflect a minor contamination of epithelial cells with contractile cells, most likely ISEMFs, which are closely opposed to the epithelium. RT-PCR was then used to query each fraction for specific molecules involved in the Hh signal transduction cascade (Fig. 1F). *Shh* and *Ihh* mRNAs are restricted to the epithelium, while *Ptch1*, *Ptch2*, all three Gli transcription factors, and two known Hh target genes (*Bmp4* and *Hhip*) are exclusively expressed in the mesenchyme. Thus, the combined evidence strongly

indicates that Hh signals in the neonatal small intestine follow a paracrine route.

Blockade of Hh signals in villin-*Hhip* mice

Hhip attenuates Hh activity by binding to all Hh proteins with high affinity (Chuang and McMahon, 1999). The phenotype of *Hhip*$^{-/-}$ mice is consistent with increased Hh signaling (Chuang et al., 2003; Kawahira et al., 2003), while overexpression of *Hhip* mirrors loss of Hh signaling (Chuang and McMahon, 1999). The *Hhip* cDNA used in the villin-*Hhip* transgene contains a deletion of the C-terminal 22 amino acid transmembrane domain; this secreted form of the Hhip protein is an effective inhibitor of Shh as well as Ihh signaling, *in vitro* and *in vivo* (Chuang and McMahon, 1999; Treier et al., 2001).

The mouse villin promoter directs high-level transgene expression exclusively in the intestinal epithelium as early as E12.5, and is largely resistant to chromosomal position effects (Madison et al., 2002). Our study of villin-*Hhip* transgenic mice encompassed analysis of 18 independent founders, 14 of which demonstrated a phenotype, though the level of transgene expression varied widely (Fig. 1G,H, top). Villin-*Hhip* mice exhibited a variable, but significant reduction of two direct transcriptional targets of Hh signals (*Ptch1* and *Gli1*) for all eight founders assayed (Fig. 1H, bottom), confirming that HhipΔTM overexpression attenuated Hh signaling to varying degrees.

Reduction in Hh signaling affects villus morphogenesis and epithelial proliferation

Villin-*Hhip* founders were sacrificed at P0, P2, P3, or P5, and intestines were examined histologically. In the three founders expressing the highest levels of the transgene and exhibiting over 75% reduction in *Ptch1* mRNA (Founders #4, 5, 6, Fig. 1H) the epithelium was flattened (Fig. 2B-D). Ki67 staining revealed that the flattening was not due to loss of proliferative cells; rather, the epithelium was hyperproliferative (Fig. 2F-H) and in some regions, exhibited a pseudostratified rather than simple columnar form (Fig. 2F, arrows, insets). In some areas from high-expressing (but not low-expressing) founders, the muscularis externa was severely reduced (see Fig. 4I), a feature also observed, though to lesser extent, in *Ihh* and *Shh* null mice (Ramalho-Santos et al., 2000). Hyper-proliferation and stratification of the epithelium concomitant with blunted villi suggests that strong attenuation of Hh signaling interferes with epithelial remodeling and villus formation in the fetal small intestine.

In general, mice that survived beyond P0 expressed lower

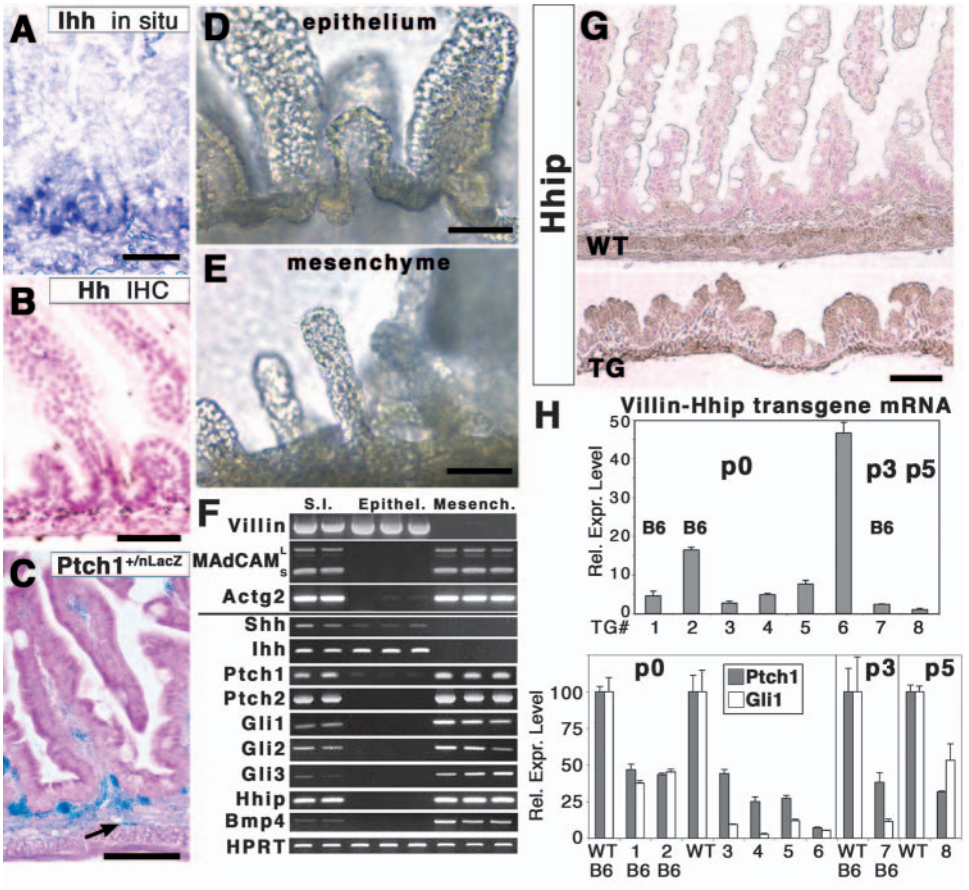

Fig. 1. Hh signaling in the neonatal small intestine is paracrine. Hh signals are attenuated in villin-*Hhip* mice. (A) In situ hybridization for *Ihh* in E18.5 small intestine shows predominant expression in intervillus epithelium. (B) Immunohistochemical staining (brown) for Shh and Ihh with anti-Hh antibody reveals Hh protein in lamina propria at the villus base. (C) X-gal stain of small intestine from a P0 *Ptch1*$^{+/nLacZ}$ mouse demonstrates that subepithelial mesenchymal cells and scattered SMCs in the ME closest to the epithelium (arrow) respond to Hh signals. (D,E) Isolated epithelium (D) and mesenchyme (E) from E18.5 small intestine. (F) RT-PCR analysis of known epithelial (villin) and mesenchymal (*Madcam1*, *Actg2*) markers demonstrates the purity of each fraction. *Shh* and *Ihh* mRNAs are exclusively epithelial, while *Ptch1*, *Ptch2*, *Gli1, Gli2*, *Gli3*, *Hhip*, and *Bmp4* are mesenchymal. Each RT-PCR was done on three independently isolated fractions and total small intestine (S.I.). *HPRT* levels appear uniform. (G) Immunostain for Hhip (brown) in P0 wild-type small intestine (WT, top) shows expression in submucosa and muscularis externa of newborn jejunum. P0 villin-*Hhip* mice (TG, bottom) exhibit ectopic expression of Hhip in the epithelium. (H, top) Q-RT-PCR for the villin-*Hhip* transcript reveals a 45-fold range of expression of the transgene in P0-P5 jejunum from eight founders. villin-*Hhip* mRNA levels are expressed relative to founder #8, set equal to 1.0. (H, bottom) Q-RT-PCR shows that Hh-inhibition results in significant downregulation of Hh target genes, *Ptch1* and *Gli1*, relative to wild-type littermates (set at 100%). Q-RT-PCR data are normalized to threshold cycle values for *HPRT*. Error bars equal s.e.m. for triplicate analysis. Founders are either on C57BL/6 background (indicated as B6), or hybrid background (B6×SJL). Scale bars: 50 μm.

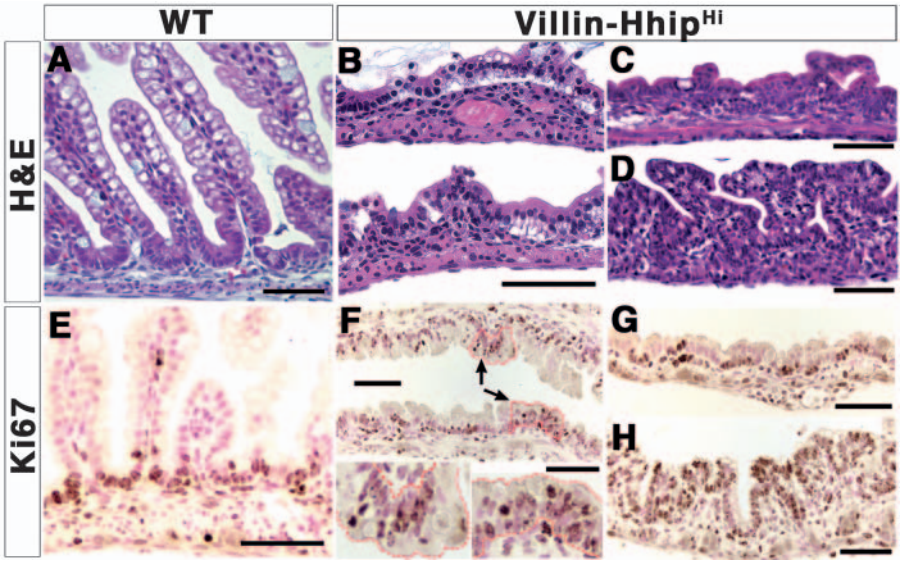

Fig. 2. High-level Hh inhibition interferes with epithelial remodeling and villus formation. (A-D) H-E staining. (A) Wild-type animals exhibit organized and well-developed villi. (B-D) Founders #4, 5, 6 (villin-*Hhip*^{Hi}) display regions of flattened epithelium. (E-H) Ki67 staining for proliferative cells (brown nuclei). (E) In wild-type mice, Ki67 positive cells are restricted to the intervillus base. The flattened epithelium of founders #4 (F), #5 (G) and #6 (H) is highly proliferative. Stratified epithelium is also evident in these founders (F, arrows, insets). Scale bars: 50 μm for A-H; 20 μm for F.

levels of the transgene (Fig. 1H) and exhibited milder phenotypes. Remarkably, even mice expressing low levels of HhipΔTM displayed disorganization of villus architecture. Structures resembling nascent crypts were seen on the sides of oddly shaped, thickened, and often branched villi (Fig. 3A-D). Proliferation was extensive throughout the villus epithelium (Fig. 3C), and epithelial nuclei in ectopic crypt structures were Ki67 positive (Fig. 3D). In wholemount preparations, extensively branched tree-like structures were observed (Fig. 3F).

Enterocyte differentiation is compromised in the intestinal epithelium of villin-*Hhip* mice

The dramatic increase in epithelial proliferation seen in villin-*Hhip* mice led us to examine the differentiation state of villus epithelial cells. As detected by immunostaining, iFABP protein was absent in broad areas of villus tip epithelium (Fig. 4B). In serial sections stained either for iFABP or Ki67, staining was reciprocal; regions positive for iFABP were largely negative for Ki67 (compare Fig. 4B to Fig. 4C). This staining pattern emphasizes the disorganization of the villus, and reveals loss of the polarity normally seen in wild-type mice in which proliferative cells are always restricted to the villus base (Fig. 2E). villin-*Hhip* mice also exhibited reduced levels of cGMP-dependent protein kinase II (*Prkg2/cGKII*), a brush border kinase, normally expressed on villus tips (Fig. 4E) (Jarchau et al., 1994).

As intestinal cells differentiate along the crypt-villus axis, the apical brush border matures; F-actin becomes more concentrated at the apical surface (Stappenbeck and Gordon, 2000) and microvilli increase in length. In high-expressing founders, electron microscopy revealed a poorly developed brush border on villus tips (Fig. 4G). Brush border-associated F-actin was significantly reduced (Fig. 4I,J). Together, these data indicate that the normal program of cellular differentiation along the crypt-villus axis is compromised in villin-*Hhip* mice. Defects in enterocyte function (and thus nutrient absorption) could contribute to neonatal wasting of villin-*Hhip* mice.

Though earlier studies documented somewhat reduced numbers of cholecystokinin (CCK) cells in *Ihh*$^{-/-}$ mice, these

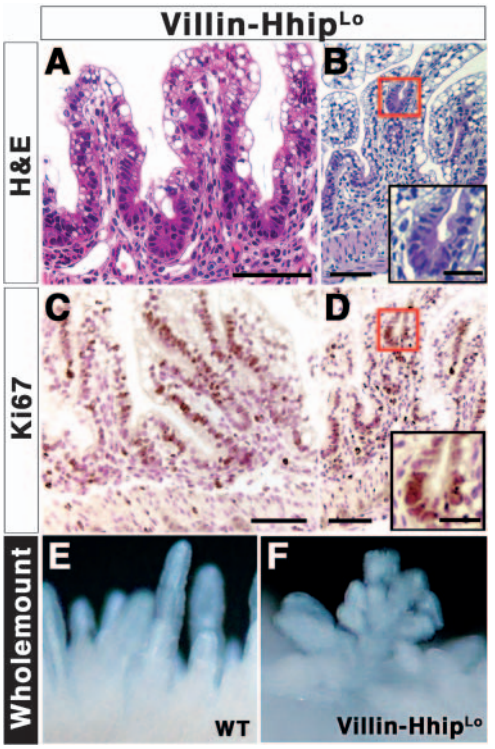

Fig. 3. Low-level Hh inhibition causes abnormal villus patterning and increased epithelial proliferation (A,B) H-E staining shows that villin-*Hhip* mice demonstrate broad extensively branched villi. Ectopic precrypt structures are seen on villus tips (A,B, inset). (C,D) Ki67 staining. The epithelium is highly proliferative (brown nuclei). Ectopic crypt-like structures contain proliferating cells (D, inset). (E,F) Wholemount view of villus structures. Wild-type P3 duodenum contains characteristic finger-like villi (E), whereas villin-*Hhip* P3 founders exhibit extensively branched villus structures (F). Scale bars: 50 μm (20 μm for insets in B and D).

cells were normally represented in villin-*Hhip* mice, as were goblet cells (see Fig. S1A-F in the supplementary material). Similarly, while alterations in the number or positioning of

enteric neurons were observed in both *Shh*$^{-/-}$ and *Ihh*$^{-/-}$ models, no obvious changes in neuronal patterning were observed in villin-*Hhip* mice (Fig. 4I,J). This latter discrepancy may be explained by temporal differences. Since differentiated enteric neurons can be found in mouse intestine as early as E10.5 (Young et al., 1999) and the villin promoter drives expression no earlier than E12.5 (Madison et al., 2002), neuronal differentiation probably precedes HhipΔTM expression. Together, the data indicate that enteric neurons, once established, can be maintained in the presence of reduced Hh signals.

Villin-*Hhip* mice exhibit increased Tcf4/β-catenin activity in the intestinal epithelium

The Wnt pathway, through its control of target genes such as c-*myc*, regulates the master switch between proliferation vs. differentiation in the intestinal epithelium (Pinto et al., 2003; van de Wetering et al., 2002). Clearly, this switch is perturbed in villin-*Hhip* mice. Wnt signals are also critical for maintenance of the crypt compartment (van de Wetering et al., 2002) and villin-*Hhip* mice exhibit an increase in precrypt-like structures. Finally, branched villi, in association with increased epithelial proliferation, were also seen in transgenic mice in which the canonical Wnt pathway was enhanced by overexpression of a constitutively active form of β-catenin in the intestinal epithelium (Wong et al., 1998). All of these features prompted us to examine markers of epithelial Wnt signaling in the villin-*Hhip* model. In wild-type mice, known Tcf4/β-catenin target genes (*Cdx1*, *Cd44* and *Ephb2*) are normally restricted to the crypt compartment (Batlle et al., 2002; Lickert et al., 2000; Wielenga et al., 1999). All three of these markers were highly expressed throughout the epithelium of transgenic founders (Fig. 5B,D,F). In P2 to P5 transgenic mice, increased expression of these markers was apparent in the ectopic crypt-like structures (Fig. 5D,F, insets). The *c-myc* proto-oncogene, a known Tcf4/β-catenin target, was also significantly upregulated (Fig. 5G). To further investigate this apparent increase in canonical Wnt signaling, we examined the intracellular localization of β-catenin. In normal villus tip cells, where Wnt signals are low or absent, β-catenin is membrane associated. In contrast, intervillus epithelial cells display cytoplasmic and nuclear β-catenin, reflecting Wnt activity (Fig. 5I, arrows). In villin-*Hhip* mice this pattern is perturbed: increased levels of cytoplasmic and nuclear β-catenin are observed, even in villus tip epithelial cells (Fig. 5J,K, arrows).

Intestinal myofibroblasts respond to Hh signals and are mislocated in villin-*Hhip* mice

ISEMFs can influence epithelial proliferation (Powell et al., 1999) and represent a possible source of Wnt ligands that drive proliferation in the epithelial crypt compartment (Brittan and Wright, 2004; van de Wetering et al., 2002). Since pericryptal ISEMFs are in close proximity to epithelially secreted Shh and Ihh, we examined their potential to respond to Hh signals. First, we examined four ISEMF cell lines, derived from different regions of rat or human intestine (Plateroti et al., 1998; Valentich et al., 1997), for target gene expression in response to Shh-conditioned medium. All lines indeed respond to Hh signals by upregulation of the canonical target genes, *Gli1* and *Ptch1* (Fig. 6A,B). ISEMFs can be identified in tissue by their expression of alpha-smooth muscle actin (α-SMA), a marker that is largely absent from other fibroblasts of the villus tip lamina propria (Adegboyega et al., 2002; Sappino et al., 1989). In addition, ISEMFs are negative for desmin, a marker of

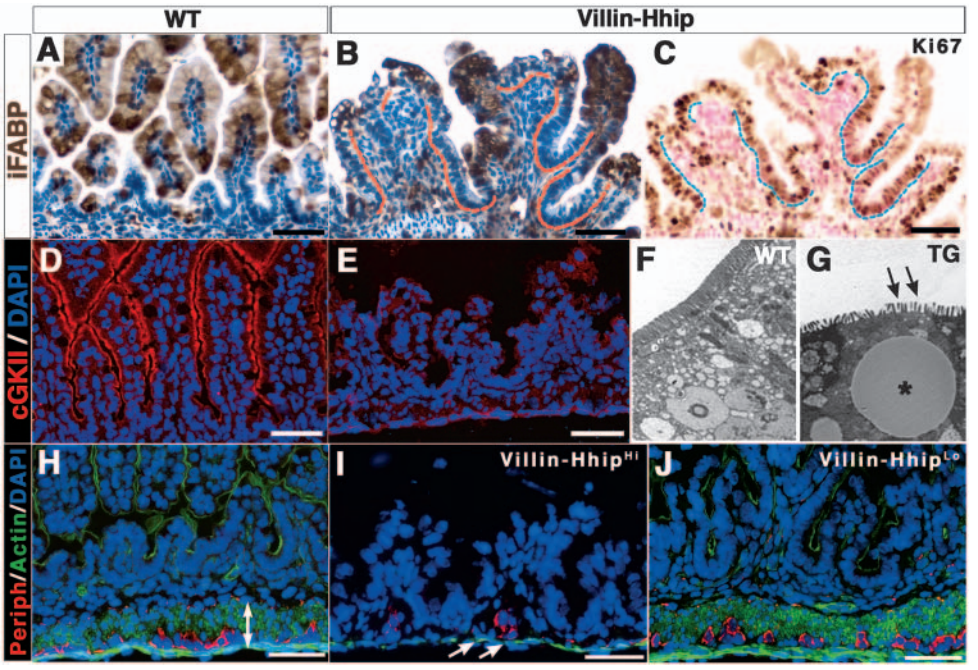

Fig. 4. Hh signals are required for proper enterocyte differentiation. (A) The enterocyte marker, iFABP, is expressed only in differentiated villus tip epithelium in P0 wild-type small intestine (brown). (B) In P0 transgenic small intestine, iFABP is missing from broad regions of villus epithelium (red dotted line). (C) Ki67 immunostaining of a section adjacent to the one shown in B reveals that regions lacking iFABP contain proliferating cells (blue dotted line). (D) The brush border kinase, cGKII (red), is expressed at the apical surface of differentiated epithelial cells, as seen in wild-type P0 mice. (E) cGKII expression is severely reduced in villin-*Hhip* P0 mice. (F) Transmission electron microscopy of villus tip epithelial cells from wild-type P0 small intestine reveals a well-formed brush border. (G) Villin-*Hhip* mice have a shortened, poorly formed brush border (arrows) and large lipid droplets are seen at the apical end of epithelial cells (asterisk). (H-J) Immunofluorescence staining for actin (green) stains the epithelial brush border and smooth muscle of the small intestine; the neuronal marker peripherin (red) stains enteric neurons. (H) Wild-type P0. (I) In high-expressing founders, neuronal cells are well represented, but muscle layers are obviously reduced (arrows). Brush border actin staining is negligible. (J) Low-expressing founders exhibit normal peripherin staining and normal musculature. A-I are from neonates and J is from P5 mouse. Scale bars: 50 μm.

smooth muscle cells (SMCs) (Adegboyega et al., 2002). Confocal microscopy reveals that in P0 *Ptch1*$^{+/nLacZ}$ mice, subepithelial cells with LacZ-positive nuclei express α-SMA, but not desmin (Fig. 6C-F). Scattered SMCs of the innermost layer of the ME (Fig. 6C,D, arrowhead) and rare desmin(+)/α-SMA(–) cells also exhibited LacZ-positive nuclei (Fig. 6F, arrowhead).

We next examined the distribution of ISEMFs and SMCs in the stromal compartment of wild-type vs. villin-*Hhip* small intestines. In wild-type mice, α-SMA-positive, desmin-negative ISEMFs are found in close association with the epithelium in the precrypt region (Fig. 7A,C). In central regions of villus cores, ISEMFs are found in fewer numbers (Fig. 7A,B). In contrast, in villin-*Hhip* founders, ISEMFs are located in close apposition to the epithelium of the villus tips (Fig. 7D-I). Proliferative epithelium is often seen immediately adjacent to ectopic ISEMFs (Fig. 7F, arrows), suggesting that signals from these ectopically located cells could be responsible for the proliferative response of the epithelium. In addition, numerous desmin-positive, α-SMA-negative (or low) cells occupied the broadened villus cores of low-expressing founders (Fig. 7D,E,G,H). Since desmin is the earliest structural muscle-specific protein seen during muscle development (Brand-Saberi and Christ, 1999; Capetanaki et al., 1997; Olson, 1990; Weintraub et al., 1991), these cells are likely to be immature SMCs. Thus, even slight reductions in Hh signaling alter the organization of stromal cell subpopulations in villus tip lamina propria; desmin-positive SMCs are expanded and ISEMFs, typically concentrated in intervillus regions of wild-type mice, are abnormally located beneath villus tip epithelium. These mesenchymal patterning defects secondarily perturb epithelial organization along the crypt-villus axis.

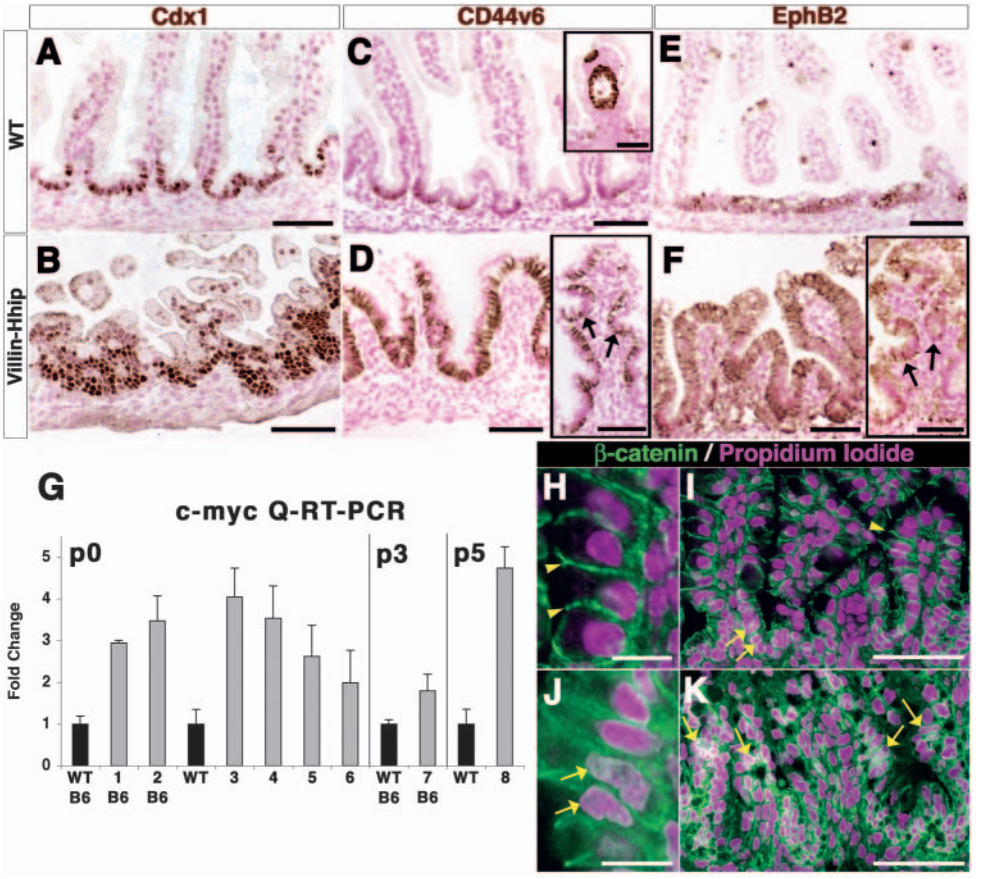

Fig. 5. Tcf4/β-catenin activity is enhanced in villin-*Hhip* mice. (A,C,E) Wild-type mice. (B,D,F) villin-*Hhip* mice. Tcf4/β-catenin target genes *Cdx1* (A), *Cd44* (C), and *Ephb2* (E) are normally present in the wild-type P0 intervillus epithelium. *Cd44* is upregulated in polyps, as seen in this spontaneous lesion in wild-type duodenum (C, inset). In P0 villin-*Hhip* mice, *Cdx1* (B), *Cd44* (D), and *Ephb2* (F), expression domains are expanded onto villus tip epithelium. *Cd44* and *Ephb2* expression is also evident in ectopic crypt-like structures in this P3 mouse (D,F, inset, arrows). (G) Q-RT-PCR of P0, P3, P5 jejunum RNA for *c-myc* mRNA. All founders had significant increases in *c-myc* expression levels, relative to WT (set equal to 1.0). Error bars represent s.e.m. for triplicate analysis. Overlap of β-catenin (green) and propidium iodide (magenta) is seen as white. Note that in P0 wild-type mice, β-catenin is present exclusively at cell-cell junctions in villus tip epithelium (H, arrowheads), while nuclear β-catenin (white) is restricted to proliferating cells in intervillus regions (I, arrows). In P0 villin-*Hhip* transgenic mice, increased levels of cytoplasmic and nuclear β-catenin are observed in villus tip epithelium (J,K, arrows). Scale bars: 50 μm for A-F,I,K; 100 μm for C (inset); 10 μm for H,J.

Shh induces Bmp4 expression, but Bmp signals are not solely responsible for establishment of villus polarity

Shh induces *Bmp4* expression in mesenchyme during intestinal development (Roberts et al., 1995; Roberts et al., 1998; Sukegawa et al., 2000), and this limits stromal growth (Smith et al., 2000). We therefore considered the possibility that the stromal and/or epithelial phenotype in villin-*Hhip* mice involves alterations in Bmp signals. Q-RT-PCR analysis revealed a moderate decrease in *Bmp2* and *Bmp4* in some founders, and a substantial decrease in *Bmp7* in all villin-*Hhip* founders compared to wild-type littermates (see Fig. S2A in the supplementary material). When we examined the location of *Bmp* mRNAs in separated fractions of E18.5 small intestinal epithelium and mesenchyme, we found that *Bmp4* is exclusively mesenchymal, *Bmp7* is predominantly epithelial, and *Bmp2* is expressed in both compartments (see Fig. S2B in the supplementary material). By exposing C57BL/6 E18.5 small intestinal mesenchyme to recombinant mouse N-terminal Shh (Shh-N), we were able to induce expression of *Bmp4* (but not *Bmp2*) in a dose-dependent manner, as early as 12 hours after stimulation (see Fig. S2C,D in the supplementary

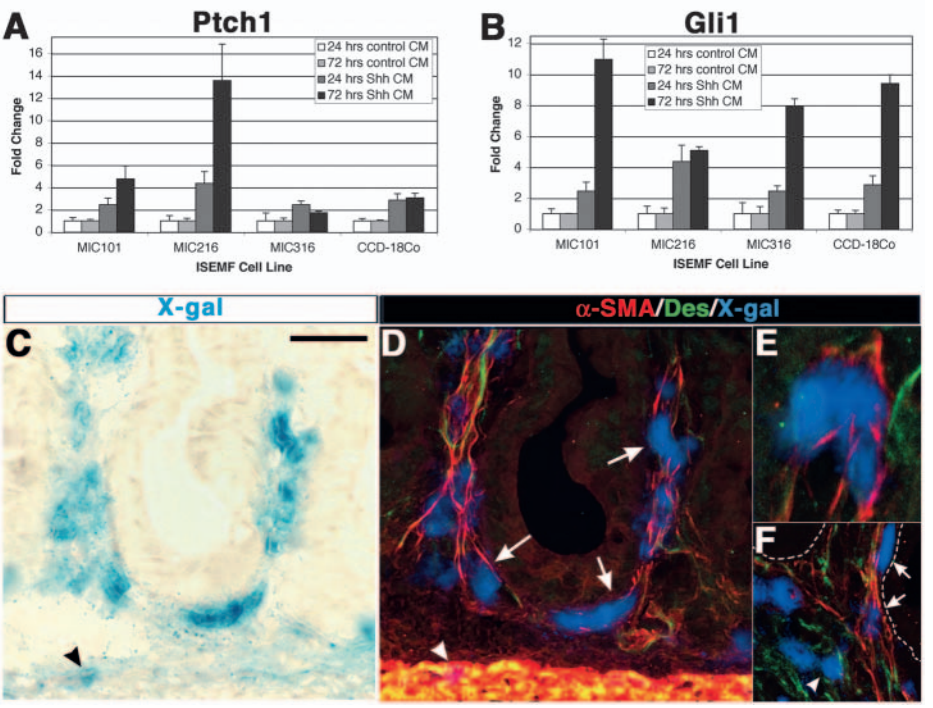

Fig. 6. ISEMFs express Ptch1 and are responsive to Shh stimulation. (A,B) ISEMF cell lines from rat jejunum (MIC101), ileum (MIC216), colon (MIC316), and human colon (CCD-18Co) respond to 24- or 72-hour treatment with Shh-conditioned medium (CM) from Cos7 cells transfected with pcDNA3.1-Shh (Shh CM) or pcDNA3.1 (control CM). Q-RT-PCR analysis reveals upregulation of Gli target genes *Ptch1* (A) and *Gli1* (B). Error bars represent s.e.m. of triplicate analysis. (C) X-gal stain marks nuclear LacZ expression from *Ptch1* locus in cells beneath intervillus epithelium in P0 $Ptch1^{+/nLacZ}$ small intestine. (D-F) Confocal microscopy of immunofluorescence for α-SMA (red) and desmin (green) identifies ISEMFs beneath epithelium. False-color overlay of X-gal stain (blue) reveals that ISEMF cells surrounding precrypts (arrows) express Ptch1. X-gal-positive nuclei are also found in scattered surface SMCs of the muscularis extrema (C,D, arrowhead) and in rare desmin-positive cells in the lamina propria (F, arrowhead). Scale bar: 20 μm.

material). Since *Bmp7* expression is epithelial, *Bmp4* is the only one of the three family members that could be a direct Hh target, whereas *Bmp2* and *Bmp7* must be indirectly altered downstream of the Hh signal. To investigate the role of Bmps in polarization of the crypt-villus axis and regulation of epithelial proliferation, we created villin-noggin mice. Noggin is a secreted polypeptide that binds to and inhibits extracellular Bmp2, 4, and 7 (Zimmerman et al., 1996). Transgenic founders were analyzed at P0, but no defects in villus polarization or epithelial proliferation were observed despite readily detectable expression of noggin protein in the epithelium (see Fig. S2E,F in the supplementary material).

Villin-noggin mice were also generated by Haramis et al. (Haramis et al., 2004). Consistent with our own findings, neonatal villin-noggin mice showed no obvious phenotype. However, after P28, these mice exhibited an expanded stromal compartment and developed ectopic crypt structures on villi – features very similar to our villin-*Hhip* mice. This ultimately leads to the formation of intraepithelial neoplastic lesions similar to those seen in patients with juvenile polyposis syndrome (JPS). It is possible that the villin-*Hhip* model, in which two signaling pathways (Bmps and Hh) are perturbed in the

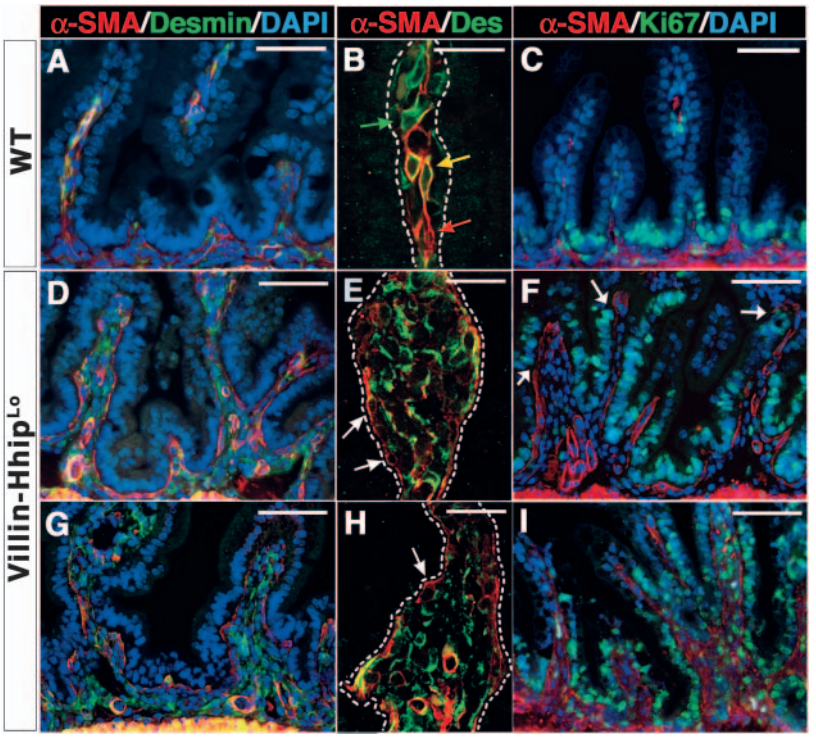

Fig. 7. Ectopic ISEMFs and expanded SMCs in villus tips of villin-*Hhip* mice. Immunofluorescence for α-SMA (A-I, red), desmin (A,B,D,E,G,H, green), or Ki67 (C,F,I, green). (A-C) Wild-type mice. Myofibroblasts (α-SMA positive, desmin negative) are primarily associated with epithelium in intervillus regions (A) and few are found in villus cores (B, red arrow). SMCs in villus tips express desmin and α-SMA (A,B, yellow arrow); SMC precursors and pericytes express desmin only (B, green arrow); Epithelial proliferation (C, green) is restricted to intervillus epithelium in WT p3 intestine. (D-I) villin-*Hhip* mice. ISEMFs are found subjacent to epithelium throughout the villus axis (D,G, red; E,H, red, arrows). The villus tip core (outlined in B,E,H) also contains an increased number of desmin-positive SMCs (D,E,G,H, green). Ectopic epithelial proliferation is often adjacent to ectopic ISEMFs (F, arrows) in P3 (F) or P5 (I) mice. Nuclei are counterstained with DAPI (blue). Scale bars: 50 μm; 20 μm for confocal images (B,E,H).

neonate, unveils an early cooperation between Bmp and Hh signals to spatially restrict formation of the crypt compartment to the intervillus base, a function that may be mainly served by Bmps alone later in life.

Discussion

Through attenuation of both Shh and Ihh signaling across a broad range of HhipΔTM expression levels, we have discovered new roles for the combined Hh signal in villus formation and crypt-villus patterning. Several aspects of the phenotype observed in villin-*Hhip* mice (epithelial hyperplasia, ectopic precrypt structures, mislocalized ISEMFs, and villus branching) were not seen in either the *Shh* or *Ihh* null models. Some aspects do mirror results seen in an earlier study in which Hh signaling was partially inhibited in neonatal pups via injection of an anti-Hh antibody, though a detailed molecular analysis was not carried out in that study (Wang et al., 2002). Thus, while the ratio of remaining Shh/Ihh ligands is not known, the phenotypes are not likely to reflect a specific reduction in either Shh or Ihh alone, but instead point to functions of the combined signal. Through this combined Hh signal, the epithelium indirectly controls the size and location of its own Wnt-responsive proliferative compartment, thus establishing the regular polarity of the villus axis prior to crypt emergence.

Hh signals impact subepithelial myofibroblasts

ISEMFs actively participate in epithelial-mesenchymal crosstalk, regulating both epithelial proliferation and differentiation (reviewed by Kedinger et al., 1998; Powell et al., 1999). Though normally concentrated in pericryptal regions, ISEMFs can be mobilized by chemotactic signals such as TGFβ, endothelin 1, and PDGF-BB, and this is important during injury repair (De Wever and Mareel, 2003; Marra et al., 1999; Powell et al., 1999). In adenocarcinomas, ISEMFs are amplified (Adegboyega et al., 2002; Sappino et al., 1989), and ISEMF-derived factors are thought to be important in the proliferation, adhesion, and migration of tumor cells (Bhowmick et al., 2004; Dignass et al., 1994). The work presented here shows that ISEMFs represent a major target for Hh signaling in the intestine. In villin-*Hhip* mice, these cells are abnormally distributed in villus tips, in close association with ectopic proliferating epithelial cells and mislocalized precrypt structures. Thus, we conclude that Hh signals sent to epithelially associated ISEMFs localize the precrypt structure and maintain the organization of the crypt-villus axis.

Mitogenic and inhibitory effects of Hh on intestinal smooth muscle (SM) patterning

Besides ISEMFs, two additional cell types in the intestinal mesenchyme respond to Hh as measured by Ptch1$^{+/nLacZ}$ staining: SMCs of the innermost layer of the ME; and α-SMA(–)/desmin(+) cells within the lamina propria. The SM phenotypes of villin-*Hhip* mice may reflect alterations in both these populations; transgene expression level also clearly plays a role in these differential responses. In mice with high levels of HhipΔTM, the ME is severely reduced. This reduction is more severe than is seen in either *Shh*$^{-/-}$ or *Ihh*$^{-/-}$ mice, suggesting that Shh and Ihh play cooperative mitogenic roles in the development of this structure. Previous studies in the kidney (Yu et al., 2002), lung (Miller et al., 2004; Weaver et al., 2003) and gut (Roberts et al., 1998; Smith et al., 2000) are consistent with a mitogenic effect of Hh signals on SM progenitors. In villin-*Hhip* mice with mild reductions in Hh signaling, desmin(+)/α-SMA(–) or α-SMA(lo) cells (probably immature SMC) are expanded in villus core lamina propria. This suggests that Hh acts to inhibit the proliferation or differentiation of SM in this compartment. In fact, epithelial Hh has been shown to direct the circumferential patterning of chick gut by inhibiting SM differentiation in the proximal lamina propria, thereby ensuring the development of the ME only in the outermost layers of the gut tube (Sukegawa et al., 2000). Both mitogenic and inhibitory effects of Hh have also been demonstrated in the kidney (Yu et al., 2002). In the villin-*Hhip* model, these effects are dose dependent and could reflect the morphogenic effects of Hh (Tabata and Takei, 2004), or may be secondary to the timing of transgene expression (the transgene is activated earlier in high expressors). However, since two SM cell types of the ME and the lamina propria are Hh targets, the apparently opposite responses may reflect cell-intrinsic differences, perhaps modified by the distinct cellular neighborhoods inhabited by these cells.

Hh signals and epithelial patterning

The effects of Hh attenuation on the epithelium are dramatic. These effects are indirect – the result of altered secondary signals from the mesenchyme. Mice expressing the highest levels of HhipΔTM exhibit an immature epithelium with poorly formed villi and impaired conversion from a pseudostratified epithelium to a simple columnar morphology. Previous studies in the mouse have demonstrated that villus morphogenesis is partially coordinated through epithelial secretion of platelet-derived growth factor A (PDGFA), which stimulates mesenchymal condensation, proliferation, and evagination of overlying epithelium to form villi (Karlsson et al., 2000). However, *Pdgfa* null mice do not demonstrate complete loss of villi. It is possible that Hh and PDGF, both epithelial signals, cooperate to mediate this mesenchymally driven remodeling process.

Our studies further demonstrate that subsequent to villus formation, Hh signals are required to organize the crypt-villus axis such that the proliferative compartment is properly localized to the intervillus base. Interestingly, though the epithelial cells expressing Hh are the same cells that normally proliferate in response to Wnt signals (Korinek et al., 1998; Pinto et al., 2003), our results reveal that Hh signals are not required for epithelial proliferation, maintenance of epithelial Wnt target gene activity, or for formation of precrypt structures, since all of these activities are stimulated in villin-*Hhip* mice. In light of the concurrent finding of mislocalized ISEMFs in villin-*Hhip* mice, we speculate that reduced Hh levels may interfere with an anchoring activity responsible for restricting the precrypt cells to the intervillus region. Though details of this anchoring mechanism are not complete, these studies clearly demonstrate that Hh-mediated paracrine signaling is responsible for organizing the proliferative compartment of the intestinal epithelium. It is intriguing that while both the adult colon and neonatal small intestine both employ Hh signals to restrict epithelial proliferation and Wnt target gene activity, this action is mediated by very different routes (van den Brink et al., 2004). In the colon, *Ihh* and *Tcf4*

mRNAs are found in two different cellular compartments (differentiated and proliferative cells, respectively) and the two signaling pathways mutually repress each other in a manner that requires autocrine signaling by Ihh.

Hh signaling and tumorigenesis

We demonstrate here that epithelial proliferation in the neonatal small intestine is highly sensitive to the level of Hh signaling. This predicts that alterations in components of the Hh pathway that lead to reduced Hh signaling could potentially predispose to tumors. That is, in a slight twist to the original Kinzler and Vogelstein description (Kinzler and Vogelstein, 1998), the epithelial Hh signal has an 'auto-landscaper' effect via its control of mesenchymal to epithelial crosstalk. The pro-proliferative effect of reduced Hh signaling appears contrary to recent findings that in several other endodermally derived organs (lung, stomach, biliary tree, and pancreas), overexpression of Hh ligands in the epithelium is associated with cancer (Berman et al., 2003; Thayer et al., 2003; Watkins et al., 2003). Importantly, these tumors rely on Hh ligands for autocrine rather than paracrine stimulation of tumor growth. In fact, inhibition of Hh signals has been proposed as a potential therapy for these aggressive tumors (Berman et al., 2003; Thayer et al., 2003; Watkins et al., 2003). It seems clear that reduced Hh signaling activity promotes epithelial proliferation in both neonatal small intestine (this report) and adult colon (van den Brink et al., 2004), though this has yet to be tested in adult small intestine. Thus, therapies aimed at shrinking gastric, pulmonary, or pancreatic cancers by untargeted pharmacological inhibition of Hh could potentially augur disastrous intestinal pathology.

We gratefully acknowlege Drs. Sally Camper, Andrzej Dlugosz, Doug Engel, Ormond MacDougald, and Linda Samuelson for critical review of this manuscript. We thank Dr Debra Silberg (University of Pennsylvania), Dr Jeffrey Gordon (Washington University School of Medicine), Dr Michael Uhler (University of Michigan), and Dr Michele Kedinger (INSERM, Strasbourg, France) for generously supplying reagents. We acknowledge technical support from the University of Michigan Transgenic Core (Dr Maggie Van Keuren), the Organogenesis Morphology Core, and the Microscopy and Image-analysis Laboratory (Dr Chris Edwards). This work was supported in part by NIH P01 DK062041 (D.L.G.); B.M. was a fellow in The Organogenesis Training Program at the University of Michigan (NIH T32-HL07505).

Supplementary material

Supplementary material for this article is available at
http://dev.biologists.org/cgi/content/full/132/2/279/DC1

References

Adegboyega, P. A., Mifflin, R. C., DiMari, J. F., Saada, J. I. and Powell, D. W. (2002). Immunohistochemical study of myofibroblasts in normal colonic mucosa, hyperplastic polyps, and adenomatous colorectal polyps. *Arch. Pathol. Lab. Med.* **126**, 829-836.

Andoh, A., Fujino, S., Okuno, T., Fujiyama, Y. and Bamba, T. (2002). Intestinal subepithelial myofibroblasts in inflammatory bowel diseases. *J. Gastroenterol.* **37**, 33-37.

Batlle, E., Henderson, J. T., Beghtel, H., van den Born, M. M., Sancho, E., Huls, G., Meeldijk, J., Robertson, J., van de Wetering, M., Pawson, T. et al. (2002). Beta-catenin and TCF mediate cell positioning in the intestinal epithelium by controlling the expression of EphB/ephrinB. *Cell* **111**, 251-263.

Berman, D. M., Karhadkar, S. S., Maitra, A., Montes de Oca, R., Gerstenblith, M. R., Briggs, K., Parker, A. R., Shimada, Y., Eshleman, J. R., Watkins, D. N. et al. (2003). Widespread requirement for Hedgehog ligand stimulation in growth of digestive tract tumours. *Nature* **425**, 846-851.

Bhowmick, N. A., Chytil, A., Plieth, D., Gorska, A. E., Dumont, N., Shappell, S., Washington, M. K., Neilson, E. G. and Moses, H. L. (2004). TGF-beta signaling in fibroblasts modulates the oncogenic potential of adjacent epithelia. *Science* **303**, 848-851.

Brand-Saberi, B. and Christ, B. (1999). Genetic and epigenetic control of muscle development in vertebrates. *Cell Tissue Res.* **296**, 199-212.

Brittan, M. and Wright, N. A. (2004). The gastrointestinal stem cell. *Cell Prolif.* **37**, 35-53.

Calvert, R. and Pothier, P. (1990). Migration of fetal intestinal intervillous cells in neonatal mice. *Anat. Rec.* **227**, 199-206.

Capetanaki, Y., Milner, D. J. and Weitzer, G. (1997). Desmin in muscle formation and maintenance: knockouts and consequences. *Cell Struct. Funct.* **22**, 103-116.

Cheng, H. and Bjerknes, M. (1985). Whole population cell kinetics and postnatal development of the mouse intestinal epithelium. *Anat. Rec.* **211**, 420-426.

Chuang, P. T. and McMahon, A. P. (1999). Vertebrate Hedgehog signalling modulated by induction of a Hedgehog-binding protein. *Nature* **397**, 617-621.

Chuang, P. T., Kawcak, T. and McMahon, A. P. (2003). Feedback control of mammalian Hedgehog signaling by the Hedgehog-binding protein, Hip1, modulates Fgf signaling during branching morphogenesis of the lung. *Genes Dev.* **17**, 342-347.

De Wever, O. and Mareel, M. (2003). Role of tissue stroma in cancer cell invasion. *J. Pathol.* **200**, 429-447.

Dignass, A. U., Tsunekawa, S. and Podolsky, D. K. (1994). Fibroblast growth factors modulate intestinal epithelial cell growth and migration. *Gastroenterology* **106**, 1254-1262.

Goodrich, L. V., Milenkovic, L., Higgins, K. M. and Scott, M. P. (1997). Altered neural cell fates and medulloblastoma in mouse patched mutants. *Science* **277**, 1109-1113.

Haramis, A. P., Begthel, H., van den Born, M., van Es, J., Jonkheer, S., Offerhaus, G. J. and Clevers, H. (2004). De novo crypt formation and juvenile polyposis on BMP inhibition in mouse intestine. *Science* **303**, 1684-1686.

Jarchau, T., Hausler, C., Markert, T., Pohler, D., Vanderkerckhove, J., de Jonge, H. R., Lohmann, S. M. and Walter, U. (1994). Cloning, expression, and in situ localization of rat intestinal cGMP-dependent protein kinase II. *Proc. Natl. Acad. Sci. USA* **91**, 9426-9430.

Karlsson, L., Lindahl, P., Heath, J. K. and Betsholtz, C. (2000). Abnormal gastrointestinal development in PDGF-A and PDGFR-(alpha) deficient mice implicates a novel mesenchymal structure with putative instructive properties in villus morphogenesis. *Development* **127**, 3457-3466.

Kawahira, H., Ma, N. H., Tzanakakis, E. S., McMahon, A. P., Chuang, P. T. and Hebrok, M. (2003). Combined activities of hedgehog signaling inhibitors regulate pancreas development. *Development* **130**, 4871-4879.

Kedinger, M., Duluc, I., Fritsch, C., Lorentz, O., Plateroti, M. and Freund, J. N. (1998). Intestinal epithelial-mesenchymal cell interactions. *Ann. N.Y. Acad. Sci.* **859**, 1-17.

Kinzler, K. W. and Vogelstein, B. (1998). Landscaping the cancer terrain. *Science* **280**, 1036-1037.

Korinek, V., Barker, N., Moerer, P., van Donselaar, E., Huls, G., Peters, P. J. and Clevers, H. (1998). Depletion of epithelial stem-cell compartments in the small intestine of mice lacking Tcf-4. *Nat. Genet.* **19**, 379-383.

Lickert, H., Domon, C., Huls, G., Wehrle, C., Duluc, I., Clevers, H., Meyer, B. I., Freund, J. N. and Kemler, R. (2000). Wnt/(beta)-catenin signaling regulates the expression of the homeobox gene Cdx1 in embryonic intestine. *Development* **127**, 3805-3813.

Madison, B. B., Dunbar, L., Qiao, X. T., Braunstein, K., Braunstein, E. and Gumucio, D. L. (2002). Cis elements of the villin gene control expression in restricted domains of the vertical (crypt) and horizontal (duodenum, cecum) axes of the intestine. *J. Biol. Chem.* **277**, 33275-33283.

Marra, F., Romanelli, R. G., Giannini, C., Failli, P., Pastacaldi, S., Arrighi, M. C., Pinzani, M., Laffi, G., Montalto, P. and Gentilini, P. (1999). Monocyte chemotactic protein-1 as a chemoattractant for human hepatic stellate cells. *Hepatology* **29**, 140-148.

Mathan, M., Moxey, P. C. and Trier, J. S. (1976). Morphogenesis of fetal rat duodenal villi. *Am. J. Anat.* **146**, 73-92.

Miller, L. A., Wert, S. E., Clark, J. C., Xu, Y., Perl, A. K. and Whitsett, J.

A. (2004). Role of Sonic hedgehog in patterning of tracheal-bronchial cartilage and the peripheral lung. *Dev. Dyn.* **231**, 57-71.
Motoyama, J., Heng, H., Crackower, M. A., Takabatake, T., Takeshima, K., Tsui, L. C. and Hui, C. (1998). Overlapping and non-overlapping Ptch2 expression with Shh during mouse embryogenesis. *Mech. Dev.* **78**, 81-84.
Olson, E. N. (1990). MyoD family: a paradigm for development? *Genes Dev.* **4**, 1454-1461.
Pinto, D., Gregorieff, A., Begthel, H. and Clevers, H. (2003). Canonical Wnt signals are essential for homeostasis of the intestinal epithelium. *Genes Dev.* **17**, 1709-1713.
Plateroti, M., Rubin, D. C., Duluc, I., Singh, R., Foltzer-Jourdainne, C., Freund, J. N. and Kedinger, M. (1998). Subepithelial fibroblast cell lines from different levels of gut axis display regional characteristics. *Am. J. Physiol.* **274**, G945-G954.
Powell, D. W., Mifflin, R. C., Valentich, J. D., Crowe, S. E., Saada, J. I. and West, A. B. (1999). Myofibroblasts. II. Intestinal subepithelial myofibroblasts. *Am. J. Physiol.* **277**, C183-C201.
Prado, C. L., Pugh-Bernard, A. E., Elghazi, L., Sosa-Pineda, B. and Sussel, L. (2004). Ghrelin cells replace insulin-producing beta cells in two mouse models of pancreas development. *Proc. Natl. Acad. Sci. USA* **101**, 2924-2929.
Ramalho-Santos, M., Melton, D. A. and McMahon, A. P. (2000). Hedgehog signals regulate multiple aspects of gastrointestinal development. *Development* **127**, 2763-2772.
Roberts, D. J., Johnson, R. L., Burke, A. C., Nelson, C. E., Morgan, B. A. and Tabin, C. (1995). Sonic hedgehog is an endodermal signal inducing Bmp-4 and Hox genes during induction and regionalization of the chick hindgut. *Development* **121**, 3163-3174.
Roberts, D. J., Smith, D. M., Goff, D. J. and Tabin, C. J. (1998). Epithelial-mesenchymal signaling during the regionalization of the chick gut. *Development* **125**, 2791-2801.
Sappino, A. P., Dietrich, P. Y., Skalli, O., Widgren, S. and Gabbiani, G. (1989). Colonic pericryptal fibroblasts. Differentiation pattern in embryogenesis and phenotypic modulation in epithelial proliferative lesions. *Virchows Arch. A. Pathol. Anat. Histopathol.* **415**, 551-557.
Smith, D. M., Nielsen, C., Tabin, C. J. and Roberts, D. J. (2000). Roles of BMP signaling and Nkx2.5 in patterning at the chick midgut-foregut boundary. *Development* **127**, 3671-3681.
Stappenbeck, T. S. and Gordon, J. I. (2000). Rac1 mutations produce aberrant epithelial differentiation in the developing and adult mouse small intestine. *Development* **127**, 2629-2642.
Sukegawa, A., Narita, T., Kameda, T., Saitoh, K., Nohno, T., Iba, H., Yasugi, S. and Fukuda, K. (2000). The concentric structure of the developing gut is regulated by Sonic hedgehog derived from endodermal epithelium. *Development* **127**, 1971-1980.
Tabata, T. and Takei, Y. (2004). Morphogens, their identification and regulation. *Development* **131**, 703-712.
Thayer, S. P., di Magliano, M. P., Heiser, P. W., Nielsen, C. M., Roberts, D. J., Lauwers, G. Y., Qi, Y. P., Gysin, S., Fernandez-Del Castillo, C., Yajnik, V. et al. (2003). Hedgehog is an early and late mediator of pancreatic cancer tumorigenesis. *Nature* **425**, 851-856.
Theodosiou, N. A. and Tabin, C. J. (2003). Wnt signaling during development of the gastrointestinal tract. *Dev. Biol.* **259**, 258-271.
Treier, M., O'Connell, S., Gleiberman, A., Price, J., Szeto, D. P., Burgess, R., Chuang, P. T., McMahon, A. P. and Rosenfeld, M. G. (2001). Hedgehog signaling is required for pituitary gland development. *Development* **128**, 377-386.
Valentich, J. D., Popov, V., Saada, J. I. and Powell, D. W. (1997). Phenotypic characterization of an intestinal subepithelial myofibroblast cell line. *Am. J. Physiol.* **272**, C1513-C1524.
van de Wetering, M., Sancho, E., Verweij, C., de Lau, W., Oving, I., Hurlstone, A., van der Horn, K., Batlle, E., Coudreuse, D., Haramis, A. P. et al. (2002). The beta-catenin/TCF-4 complex imposes a crypt progenitor phenotype on colorectal cancer cells. *Cell* **111**, 241-250.
van den Brink, G. R., Bleuming, S. A., Hardwick, J. C., Schepman, B. L., Offerhaus, G. J., Keller, J. J., Nielsen, C., Gaffield, W., van Deventer, S. J., Roberts, D. J. et al. (2004). Indian Hedgehog is an antagonist of Wnt signaling in colonic epithelial cell differentiation. *Nat. Genet.* **36**, 277-282.
Wang, L. C., Nassir, F., Liu, Z. Y., Ling, L., Kuo, F., Crowell, T., Olson, D., Davidson, N. O. and Burkly, L. C. (2002). Disruption of hedgehog signaling reveals a novel role in intestinal morphogenesis and intestinal-specific lipid metabolism in mice. *Gastroenterology* **122**, 469-482.
Watkins, D. N., Berman, D. M., Burkholder, S. G., Wang, B., Beachy, P. A. and Baylin, S. B. (2003). Hedgehog signalling within airway epithelial progenitors and in small-cell lung cancer. *Nature* **422**, 313-317.
Weaver, M., Batts, L. and Hogan, B. L. (2003). Tissue interactions pattern the mesenchyme of the embryonic mouse lung. *Dev. Biol.* **258**, 169-184.
Weintraub, H., Davis, R., Tapscott, S., Thayer, M., Krause, M., Benezra, R., Blackwell, T. K., Turner, D., Rupp, R., Hollenberg, S. et al. (1991). The myoD gene family: nodal point during specification of the muscle cell lineage. *Science* **251**, 761-766.
Wells, J. M. and Melton, D. A. (1999). Vertebrate endoderm development. *Annu. Rev. Cell Dev. Biol.* **15**, 393-410.
Wielenga, V. J., Smits, R., Korinek, V., Smit, L., Kielman, M., Fodde, R., Clevers, H. and Pals, S. T. (1999). Expression of CD44 in Apc and Tcf mutant mice implies regulation by the WNT pathway. *Am. J. Pathol.* **154**, 515-523.
Wong, M. H., Rubinfeld, B. and Gordon, J. I. (1998). Effects of forced expression of an NH2-terminal truncated beta-Catenin on mouse intestinal epithelial homeostasis. *J. Cell Biol.* **141**, 765-777.
Young, H. M., Ciampoli, D., Hsuan, J. and Canty, A. J. (1999). Expression of Ret-, p75(NTR)-, Phox2a-, Phox2b-, and tyrosine hydroxylase-immunoreactivity by undifferentiated neural crest-derived cells and different classes of enteric neurons in the embryonic mouse gut. *Dev. Dyn.* **216**, 137-152.
Yu, J., Carroll, T. J. and McMahon, A. P. (2002). Sonic hedgehog regulates proliferation and differentiation of mesenchymal cells in the mouse metanephric kidney. *Development* **129**, 5301-5312.
Zimmerman, L. B., de Jesus-Escobar, J. M. and Harland, R. M. (1996). The Spemann organizer signal noggin binds and inactivates bone morphogenetic protein 4. *Cell* **86**, 599-606.

Table S1. Primers used in this study

Gene	Forward primer	Reverse primer	PCR product size
Villin	5′-AGATGGATGACTACCTGAAGGGC-3′	5′-CAGTCACCACCGTAGAAATGGC-3′	1027 bp
Madcam1	5′-GCACACCACTGTTCCGAATGAC-3′	5′-TGCCAATCCATAGGACGACG-3′	591 bp
Actg2	5′-GGGTGTGATGGTGGGAATGG-3′	5′-GGTGCTCTTCTGGTGCTACTC-3′	182 bp
Shh	5′-GCTGTGGAAGCAGGTTTCG-3′	5′-GGAAGGTGAGGAAGTCGCTG-3′	232 bp
Ihh	5′-CACCCCCAACTACAATCCCG-3′	5′-CCATCTTCATCCCAGCCTTCG-3′	168 bp
Ptch1	5′-TGTTGGTGTGGATGATGTC-3′	5′-TGTGAGGCTCTGTGTAGG-3′	377 bp
Ptch2	5′-TGCGTACACCTCCCAGATGTTG-3′	5′-AAGCAGATAGCCTCCTACCACACG-3′	889 bp
Gli1	5′-AGCCTGAGTCTGTGTATG-3′	5′-CACCACCAGCATGTATTG-3′	188 bp
Gli2	5′-CTCCAACCTTCTGTCATC-3′	5′-TAGTAGTATAGCGTGTTCTG-3′	297 bp
Gli3	5′-CAGATGTCAGCGAGAAGG-3′	5′-TGTAATGGAGGAATAGGAGATG-3′	391 bp
Hhip	5′-TCTGTGCTGAGGCTGGAC-3′	5′-CTGTAGGATTCTGGCTGATGAC-3′	231 bp
Villin-Hhip	5′-CAACTTCCTAAGATCTCCCAGGTG-3′	5′-GCAGCTTAAACGAGAGCATCTTCAG-3′	191 bp
Myc	5′-TGTACCTCGTCCGATTCC-3′	5′- CATCTTCTTGCTCTTCTTCAG-3′	151 bp
Bmp2	5′-GGAGGCGAAGAAAAGCAACAG-3′	5′-ACCTGGGGAAGCAGCAACAC-3′	189 bp
Bmp4	5′-AGAGCAGAGCCAGGGAACCG-3′	5′-CCAAAAGTGACCAGGAGGGG-3′	540 bp
Bmp7	5′-GTCCATCTCCGTAGTATCC-3′	5′-ACAGTAGTAGGCAGCATAG-3′	222 bp
Hprt	5′-AGTCCCAGCGTCGTGATTAGC-3′	5′-ATAGCCCCCCTTGAGCACACAG-3′	204 bp
Hu Ptch1	5′-CAGGAGGAGTTGATTGTG-3′	5′-TGGTTAGACAGGCATAGG-3′	358 bp
Hu Gli1	5′-AACTCCACAGGCATACAG-3′	5′-ATACATACGGCTTCTCATTG-3′	484 bp
Hu HPRT	5′-TGGCGTCGTGATTAGTGATG-3′	5′-AATCCAGCAGGTCAGCAAAG-3′	224 bp